Journal of Inflammation Research

Dovepress
Taylor & Francis Group

Open Access Full Text Article

ORIGINAL RESEARCH

Blockade of the Notch Pathway by Inhibition of Fucosylation Ameliorates Chondrocyte Inflammation and Extracellular Matrix Degradation

Yunheng Zhang[1,*], Maorong Liu[1,*], Xuan Wang[1,*], Nongchao Li[1,2], Xin Chang[1], Junkui Xu[1], Feng Tian[1], Xiaodong Wen[1], Cheng Liu[1], Yi Li[1]

[1]Department of Foot and Ankle Surgery, Honghui Hospital of Xi'an Jiaotong University, Xi'an, People's Republic of China; [2]The Second Clinical Medical College of Shaanxi University of Chinese Medicine, Xianyang, People's Republic of China

*These authors contributed equally to this work

Correspondence: Yi Li; Cheng Liu, Email footankle08@126.com; 925980519@qq.com

Objective: Osteoarthritis is a chronic degenerative disease characterised by damage to articular cartilage and degradation of the chondrocyte matrix. It has been shown that inflammation occurs with a variety of protein glycosylation abnormalities, among which elevated levels of fucosylation is one of the characteristics of OA. Now, the relationship between fucosylation and OA is not clear. By summarizing, we infer that elevated levels of fucosylation may affect the course of OA, possibly through the Notch signalling pathway.

Methods: In in vitro experiments, we established a cellular inflammation model on a mature human chondrocyte cell line and intervened with the inhibitor SGN-2FF. The effect of decreased levels of fucosylation on chondrocyte apoptosis was observed by methods such as Calcein-AM/PI staining and Lectin blotting. By western bolt and immunofluorescence, it was verified that the decreased level of fucosylation could affect the activity of Notch signalling pathway and reduce the release of inflammatory factors, thus alleviating inflammation. In in vivo experiments, OA rats were treated by joint cavity injection of SGN-2FF, and the treatment status was assessed by ELISA and Micro-CT analysis.

Results: We found abnormally elevated levels of fucosylation in a model of chondrocyte inflammation. Upon inhibition of fucosylation using SGN-2FF, there was a decrease in the expression of inflammation-related factors and a decrease in the number of apoptotic cells. With the decrease of fucosylation, the expression of activated Notch1 was significantly reduced, hindering the activation of Notch pathway and reducing the release of pro-inflammatory factors. Animal experiments showed that inhibition of fucoidan glycosylation could effectively reduce the expression of IL-6 and TNF-α, reduce cartilage damage and alleviate OA.

Conclusion: Inhibition of fucosylation can ameliorate chondrocyte inflammation and extracellular matrix degradation by decreasing Notch1 activity and down-regulating the expression of the Notch pathway, which can effectively alleviate the development of OA.

Keywords: osteoarthritis, fucosylation, fucosyltransferase, molecular mechanism, notch pathway

Introduction

Osteoarthritis (OA) is a chronic degenerative disease characterized mainly by damage to articular cartilage, alteration of subchondral bone, inflammatory reaction of synovium, and reduction of extracellular matrix, etc,[1] which can lead to joint pain, loss of function, etc, and has become a major cause of disability in the elderly.[2] However, the pathogenesis of OA remains unclear. The current national and international research hotspot is the imbalance doctrine of matrix metalloproteinases (MMPs) and tissue inhibitors of matrix metalloproteinases (TIMPs). Analysis of the plasma components of clinical patients reveals that plasma MMP-3 and TIMP-1 levels in patients with OA are significantly higher than those in normal subjects, and

Received: 31 January 2025
Accepted: 7 August 2025
Published: 18 August 2025

that plasma levels of MMP-3 and MMP-9 are not affected by knee OA grading.[3] That is, at the onset of osteoarthritis, chondrocytes abnormally secrete MMPs, which affects the production of TIMPs, leading to an accelerated matrix degradation process.[4] This provides strong clinical support for this doctrine. In addition, some cytokines, such as tumour necrosis factor α (TNF-α) and interleukin 1 (IL-1), are involved in the regulation of this process and play an important role in it.[5] Given the progressive and destructive mechanism of OA, hyaluronic acid (HA), the main component of synovial fluid, is degraded under the action of various MMPs, inflammatory factors, etc, which also leads to a decrease in the lubricating ability of the joints and an increase in friction, making articular chondropathy the most important feature of OA. An alternative to symptomatic treatment for OA is the injection of hyaluronic acid-based hydrogel combined with physiotherapy, which improves the bioadhesive properties of the synovial fluid and helps to lubricate and treat joints affected by OA.[6] Since the lesions mainly occur in the cartilage and the cartilage has no vascular supply and poor regenerative ability, early treatment for damaged cartilage includes autologous chondrocyte implantation (ACI) and matrix-induced autologous chondrocyte implantation (MACI),[7] autologous osteochondral transplantation (OATS) and OATS combined with bone marrow aspirate concentrate (BMAC) augmentation therapy,[8] and microfracture surgery,[9] among others. However, these treatments all have some disadvantages to a greater or lesser extent. Both OATS and ACI have contraindications for the treatment of OA, including the patient's age, depth of injury and Body Mass Index (BMI). Moreover, these therapies do not fundamentally address the problem of cartilage inflammation and cartilage extracellular matrix degradation, which urgently requires an in-depth study of the pathogenesis of OA and the search for new perspectives and methods to alleviate cartilage inflammation.

Fucosylation is an important protein glycosylation, which is a post-translational modification of proteins, and is found in N- and O-linked glycans and sugar chains, usually belonging to the terminal glycan modification.[10] Fucosylation is widely found in human physiology and pathological activities, such as: tissue cell development, angiogenesis, cell adhesion, inflammation, tumour apoptosis and metastasis.[11] Several studies have shown that OA is closely related to fucosylation.[12] T Matsuhashi et al observed changes in sialylation and fucosylation in a rabbit model of OA. It has been reported that α-1,3 fucosylation is increased in OA patients relative to normal individuals, and that fucosylation transferase (FUTs) are key enzymes that catalyse this process.[13] However, relatively few studies have been conducted on the specific relationship between fucosylation and OA and its mechanism. After compiling and summarising our findings, we found that fucose is most often added directly to proteins via the O-bonds of the serine/threonine hydroxyl groups of the epidermal growth factor-like (EGF) repeat sequences and the thrombin-sensitive protein type 1 repeat sequences (TSRs). The Notch pathway is a classically associated inflammatory signaling pathway, and a large number of EGF repeat sequences are present in the Notch1 receptor.[14,15] It is reasonable to suspect that OA and fucosylation are crosstalked through this pathway, but the relationship between activation of the Notch pathway and fucosylation, and their link to the development of OA, is unclear.

In this study, we created an inflammatory environment by inducing chondrocyte apoptosis and matrix degradation by IL-1β in vitro to mimic the occurrence of cartilage and chondrocyte inflammation in OA. We found that inflammation occurs with multiple inflammatory factors and matrix metalloproteinases showing high expression, and fucosylation was also abnormally elevated. By using small molecule chemical inhibitors and silencing the key enzyme FuT1 gene, the level of fucosylation can be reduced, while chondrocyte apoptosis and extracellular matrix degradation are reduced, and inflammation can be alleviated. To investigate the mechanism of action, we confirmed that the Notch pathway showed high expression during the progression of inflammation, and after the induction of fucosylation decline, the activated Notch1 was significantly reduced, and the expression of the Notch pathway was inhibited, which reduced the activation of its downstream targets and the release of inflammatory factors, and achieved the purpose of alleviating inflammation. For further validation, we surgically induced a rat OA inflammation model and treated it with a fucosylation inhibitor, and found that the cartilage inflammatory condition was reversed and OA was reduced in rats. Our findings provide clues for studying the role of glycosylation in the pathogenesis of OA and provide a new reference for the treatment of OA.

Materials and Methods

Construction of Animal OA Model

Forty male SD-rats were obtained from the Animal Experiment Center of Xi'an Jiaotong University. To establish the OA rat model, the rats in the OA modeling group were firstly paralyzed by a gas anesthesia machine (RWD, China) infused

with isoflurane (RWD, China), and the knee joints of the rats were debrided and disinfected bilaterally; then a longitudinal incision was made along the center of the knee joints, and the joint capsule was opened to cut off the anterior cruciate ligaments and the medial collateral ligament of the rats and to disarticulate the medial meniscus; then, the incision was rinsed with saline, and the joint capsule and outer skin were carefully closed with suture. After that, the incision area was rinsed with saline, and the joint capsule and outer skin were carefully sutured with sutures. In the sham-operated group, the joint capsule was incised in the same way to expose the joint cavity, which was rinsed with saline and sutured. After the surgical modeling, the rats were fed with normal feed and water.

Pharmacologic Interventions and Observations

After completing the surgical modelling, the OA model rats were equally divided into three groups (OA group, low-dose treatment group and high-dose treatment group), 10 rats in each group, and the rats were fed with conventional feed for 1 month, and 10 rats in the sham-operated group were selected as controls. At weeks 6, one rat from each group was executed, and samples of bilateral knee joints were obtained for fixation and decalcification, and paraffin sections were prepared for HE and SO staining to determine whether early OA had formed by observing cartilage wear and joint space narrowing. The rats in the sham-operated group (control group) and OA group were left untreated and allowed to move freely in their cages; the rats in the treatment group were randomly divided into two groups, and the intervention treatment was carried out on the bilateral knee joints of the rats using a low dose (2uM) and a high dose (5uM) of SGN-2FF, respectively. After anaesthetising the rats, the drug was administered by joint cavity injection using a micro syringe (Servicebio, China), with 100 μL of drug injected into each knee joint every 3 days. The rats of all groups were executed in batches at weeks 11–14 after treatment, and their knee joint samples were obtained and placed in 4% paraformaldehyde (PFA) (BOSTER, China) for subsequent manipulation as well as experimental testing.

ELISA Assay

Serum samples from rats in the control, OA, and treatment groups were collected at weeks 11–14 after drug intervention, measured using an enzyme-linked immunosorbent assay (ELISA) kit (Proteintech, China), and the concentrations of tumor necrosis factor α (TNF-α) and interleukin-6 (IL-6) were calculated.

Micro-CT Analysis

Rat knee joint samples were scanned using a micro-CT system (SkyScan 1176, Bruker, Belgium) after fixation with 4% PFA (BOSTER, China). The scans included articular cartilage and subchondral bone, and microtomography data were acquired based on three-dimensional morphometrics. Afterwards, we evaluated the bone volume fraction (BV/TV), mean trabecular thickness (TbTh), mean number of trabeculae (TbN), and mean trabecular spacing (TBSP) to determine the quality and strength of the bone.

Histological Analysis

After fixing the grouped rat knee samples with 4% PFA for 24 h, they were immersed in decalcification solution (BOSTER, China) using 10% ethylenediaminetetraacetic acid (EDTA) for 1 month. Each group of knee samples was cut into 5 μm tissue sections after dehydration and paraffin embedding. Cartilage degradation was determined by safranin O (S-O) staining, hematoxylin and eosin (H&E) staining, and toluidine blue (TB) staining, and differences between groups were compared. Cartilage degradation was assessed and analyzed using the Osteoarthritis Research Society International (OARSI) scoring system.

Cell Culture

The human chondrocyte cell line C28 (Zhongqiao Xinzhou, China) was cultured using DMEM/F12 medium (Servicebio, China) containing 10% Fetal Bovine Serum (FBS, Zhongqiao Xinzhou, China), 100 μg/mL penicillin (Servicebio, China), and 100 μg/mL streptomycin (Servicebio, China) in a cell culture incubator at 37°C with 5% CO2 in a cell culture incubator.

Establishment of OA Cell Models and Drug Toxicity Assays

To model OA chondrocytes, we used Interleukin-1 beta(IL-1β, ABclonal, China) to intervene with the cells to produce an inflammatory response. To characterize the effects of the used IL-1β and the therapeutic agent SGN-2FF (2FF, Targetmol, China) on the cell viability status, we inoculated the chondrocytes into 96-well plates (Servicebio, China) and cultured them for 24 hr at 37°C, 5% CO2, and then used different concentrations of IL-1β (0, 5, 10, 20, and 50 μM) and 2FF (0, 5, 10, 20, 50 μM), respectively, and then the cells were treated with different concentrations of IL-1β (the concentrations were 0, 5, 10, 20, 50 μM) and 2FF (0, 5, 10, 20, 50 μM), respectively; according to the manufacturer's instructions, a cell counting assay kit for cell viability assay was used (CCK-8, Servicebio, China), and 10 μL of CCK-8 reagent was added to each well, which was incubated for 2 h in a cell culture incubator, and finally detected at 450 nm by a multimode microplate reader (BioTek USA) to detect its absorbance at 450 nm and process the data using excel to determine the optimal acting concentration.

Cells were stimulated using the optimal concentration of IL-1β for 24 h to induce OA model; to this, different concentrations of 2FF (the concentrations were 0, 1, 2, 5, 10, 20, 50 μM) were added for therapeutic intervention, and cell viability values were detected using the above method at 12 h, 24 h, and 48 h after the intervention, respectively. The experiment was repeated three times to ensure the consistency of the results.

Calcein-AM/PI Staining

Chondrocytes in good growth status were pre-inoculated into 6-well plates, and the cells were treated as described in 2.7, and assayed using the Calcein-AM/PI Live/Dead Cell Double Staining Kit (Servicebio, China). Calcein-AM reagent, PI reagent, and assay buffer were returned to room temperature, cells were digested with 25% trypsin (Servicebio, China) and collected, centrifuged at 1000 rpm for 5 min, the supernatant was removed and washed 2 times using phosphate buffer solution (PBS, Servicebio, China), and Calcein AM/PI assay was added The cells were resuspended ($1x10^5$ cells/mL) in working solution and incubated in a cell culture incubator for 30 min, and finally observed and photographed using a fluorescence microscope (FV31S-SW, Olympus, Japan).

Cellular Mitochondrial Membrane Potential JC-1 Staining

Chondrocytes were inoculated in 6-well plates ($1x10^5/cm^2$) and cells were treated as described in 2.7 and assayed using the JC-1 Mitochondrial Membrane Potential Assay Kit (Servicebio, China). Cells were washed 2 times using JC-1 staining buffer, and 1 mL of JC-1 staining working solution (JC-1 solution, JC-1 dilution, and JC-1 staining buffer) and cell culture medium were added to each well, and the cells were incubated for 15 min under light protection at 37°C. The cells were observed and photographed with a fluorescence microscope (FV31S-SW, Olympus, Japan).

Hoechst 33342 Staining for Apoptosis Detection

Chondrocytes were inoculated into 24-well plates with built-in glass slides ($1x10^5/cm^2$), and the cells were processed as described in 2.7 and assayed using the Hoechst 33342 apoptosis staining kit (Servicebio, China). After fixation with 4% PFA for 15 min, 1 mL of Hoechst 33342 staining solution was added dropwise to each well and incubated at 37°C for 15 min at room temperature. Then the wells were washed twice with PBS, and the glass slides were removed and placed on slides (Servicebio, China), observed and photographed with a fluorescence microscope (LEICA, Germany).

Flow Cytometry

Flow cytometry was performed on chondrocytes grown well in vitro in culture. Chondrocytes were digested with 25% EDTA-free trypsin (Servicebio, China) to the cell suspension, centrifuged at 2000 rpm for 5 min, and the cells were washed twice with pre-cooled PBS at 4°C and then collected ($1x10^5$ cells/mL); the cells were mixed with Annexin V-FITC and PI (BOSTER, China) and incubated for 15 min at room temperature and protected from light. After incubation for 15 min, the cells were assayed within 1 h using a flow cytometer (ACEA, NovoCyte, USA).

Immunofluorescence Techniques

Well-grown chondrocytes were inoculated into 24-well plates ($2x10^4$ cells/well), and the cells were treated with different drugs according to the experimental needs and incubated for 24 hours. The cells were fixed with 4% PFA for 15 min, then permeabilized with 0.2% Triton X-100 (Servicebio, China) for 5 min, and finally closed with 5% BSA (BOSTER, China), so that they were incubated with the corresponding primary antibodies at 4°C overnight. The primary antibodies used in this study were: Bcl-2 (Proteintech, China), cleaved-Notch1 (NICD, ABclonal, China). On the following day, the cells were washed using TBST, and then incubated with FITC or CY3-labeled goat anti-mouse/rabbit IgG (Servicebio, China) for 1 h at room temperature protected from light, and finally the nuclei of the cells were stained using 4′,6-diamidino-2-phenylindole (DAPI) (Servicebio, China). The fluorescence intensity of the cells was observed using a fluorescence microscope and photographed and subsequently processed.

Cell Transfection Techniques

Twenty-four hours before transfection, C28 cells in good growth status were inoculated into 6-well plates (2×10^5 cells/well), and two hours before transfection, serum-free basal medium (F12) (Servicebio, China) was replaced. For starvation treatment, transfection was performed using Opti-MEM (ThermoFisher, USA) diluted si-FuT1 (Hysigen, China) (http://www.ncbi.nlm.nih.gov/gene/?term=2523), respectively, FuT1 negative control (NC) (Hysigen, China), mixed with Opti-MEM diluted Lipofectamine 2000 reagent (ThermoFisher, USA), added to the corresponding six-well plate, making the final concentration of si-FUT1 and NC 50 nM, and put into the cell culture incubator to transfect for 4 h. Then, the cell culture medium was replaced with complete medium; Cell transfection was detected using a fluorescence microscope (FV31S-SW, Olympus, Japan) and photographed after 12 h. Proteins or RNA were extracted after 24 h for Western blot or quantitative polymerase chain reaction assay.

Cellular Protein Extraction

Chondrocyte proteins were extracted after lysis of cells using RIPA lysis buffer (Proteintech, China), broad-spectrum protease inhibitor mixture (100xPIC) (Solarbio, China), and broad-spectrum protein phosphatase inhibitor mixture (All-inone, 100x) (Solarbio, China) according to the manufacturer's instructions. After centrifugation at 12,000 rpm and taking the supernatant, the protein was denatured by adding SDS-PAGE sample loading buffer (Servicebio, China) in a 95°C water bath. The protein concentration was determined using BCA protein concentration assay kit (BOSTER, China).

RNA Extraction and Quantitative Polymerase Chain Reaction

Total RNA from chondrocytes was extracted using the Rapid Cell RNA Extraction Kit (SPARKeasy, China) according to the manufacturer's instructions and the RNA concentration was measured using a NANODROP 2000 system (Thermo, USA), and the resultant RNA was reverse-transcribed using the PrimeScript™ RT Master Mix (SPARKeasy, China) (SimpliAmpTM Thermal Cycler, Applied Biosystems). The resulting RNA was then reverse transcribed using the PrimeScript™ RT Master Mix (SPARKeasy, China) (SimpliAmpTM Thermal Cycler, Applied Biosystems), and detected by quantitative polymerase chain reaction (Q-PCR) using a real-time fluorescent quantitative gene amplifier (BIO-RAD, USA). Primer sequences were retrieved from the online PrimerBank database (https://pga.mgh.harvard.edu/primerbank/index.html). Primer information is summarized in Supplementary Table 1.

Western Blotting

According to the experimental instructions, 10 μg of total cellular proteins in different subgroups were separated using SDS-polyacrylamide gel electrophoresis (SDS-PAGE method, Solarbio, China), transferred to polyvinylidene difluoride membranes (PVDF membranes, Merck, Germany), and the membranes were closed with 5% skimmed milk (Beyotime, China) for 1 h at room temperature. The membrane was allowed to incubate overnight at 4°C with antibodies obtained by solubilization with antibody diluent (Servicebio, China). The main antibodies used in this study were as follows: Notch1 (ABclonal, China), JAG1 (ABclonal, China), RBPJ (ABclonal, China), HES1 (ABclonal), IL-

6 (BOSTER, China), FuT1 (ABclonal, China), MMP9 (Proteintech, China), MMP13 (Bioss, China), Bcl-2 (Proteintech, China), Caspase-3 (Proteintech, China), and GAPDH (Abways, China). On the following day, after three washes with Tris-Buffered Saline with Tween 20 (TBST, Servicebio, China), the membranes were incubated with with horseradish peroxidase (HRP)-labeled goat anti-mouse/rabbit IgG (Servicebio, China) for 2 h with oscillation, and then washed three times, and then the membranes were incubated with Immobilon Western chemiluminescent HRP substrate (BOSTER, China) to treat the membranes and analyze the protein expression levels with a chemical imaging system assay (BIO-RAD USA).

Lectin Blotting

Forty μg of proteins were separated using 10% SDS-PAGE and transferred to a PVDF membrane (Merck, Germany), which was closed using 3% BSA and then incubated with biotin-labeled lectins at 4°C overnight. The main lectins used in this study were as follows: Lotus Tetragonolobus Lectin (LTL, VECTOR, USA), Aleuria aurantia lectin (AAL, VECTOR, USA). On the following day, after washing 3 times with TBST, the membranes were incubated with horseradish peroxidase (HRP)-labeled streptavidin (Solarbio, China) for 2 h with oscillation, and the blots were detected by a chemical imaging system. Gray scale values of selected protein bands were measured using ImageJ software (NIH).

Statistical Analysis

The experiments were performed at least three times. Our results are expressed as mean ± standard deviation (SD). ImageJ software and GraphPad Prism 9.0 were used to analyze the data. For comparison of two sets of data, *t*-test (*T*-test) was used. One-way analysis of variance (ANOVA) was used when the data satisfied homogeneity of variance and normal distribution. The Kruskal–Wallis H-test was applied to analyze non-parametric data. p-value less than 0.05 indicated statistical significance.

Results

IL-1β Treatment of Chondrocytes Leads to an Inflammatory Response and Is Accompanied by Elevated Fucosylation

For normal chondrocytes, we carefully observed their morphological characteristics and growth properties by several passaging cultures. To obtain chondrocytes with OA phenotype, we treated the cells with IL-1β. Before that, we used the CCK8 method to determine the effects of different concentrations of IL-1β on chondrocyte viability after 12, 24 and 48 hours, respectively, in order to obtain the optimal amount of IL-1β. The results showed that chondrocyte viability decreased significantly with the rise of IL-1β concentration. In order to mimic the in vivo inflammatory state as much as possible, we chose 20 ng/mL of IL-1β to stimulate the cells because this concentration is relatively mild (Figure 1A). By staining with Hoechst 33342, we could find that the number of apoptotic cells was significantly higher than that of normal cells and the morphology was changed in the stimulated chondrocytes (Figure 1B). We performed quantitative polymerase chain reaction on both groups of cells, and the results showed that the gene expression of IL-6 was significantly increased after IL-1β treatment (Figure 1C). After this, we extracted proteins from normal chondrocytes and inflammatory model cells respectively and performed Western blot analysis, which showed that interleukin-6 (IL-6) expression was elevated in the treated cells, while BCL-2[16] expression was decreased (Figure 1D and E). Therefore, we considered that this model could simulate the development of chondrocyte inflammation.

Based on the previously described relationship between fucosylation and osteoarthritis (OA), we hypothesized that fucosylation also showed high expression in the chondrocyte inflammatory system. Thus, we selected lectins with affinity for fucose: LTL and AAL, to detect fucosylation in normal and inflammatory cells. Lectins specifically recognize glycosyl groups and are commonly used to test glycosylation levels. By lectin blotting assay, we found that the multiple blotting bands (KDa) marked in the figure were darker in the inflammatory cells than in the normal cells, suggesting that more fucosylation occurred in the inflammatory cells (Figure 1F).

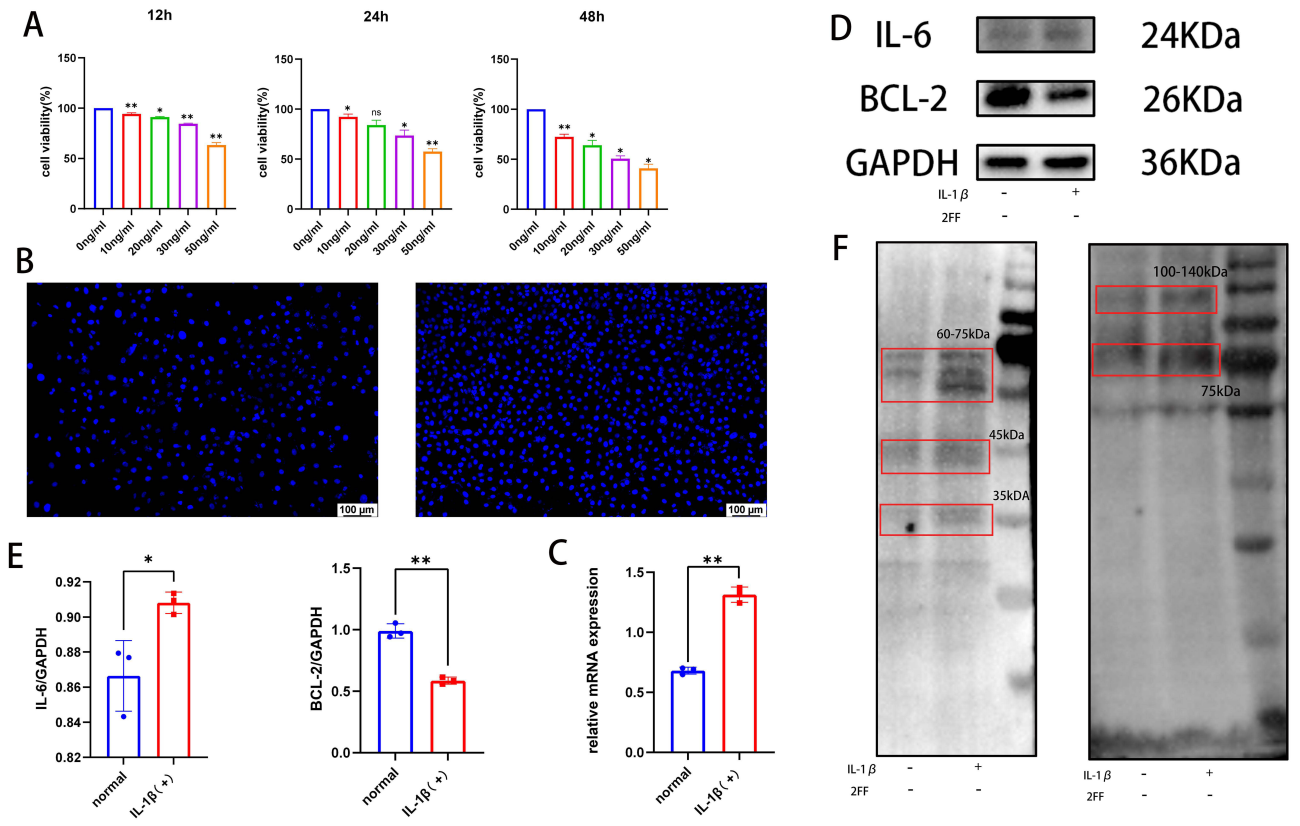

Figure 1 (**A**) Cell viability values after stimulation of chondrocytes using IL-1β, detected by CCK8 assay after 12h, 24h and 48h, respectively. (**B**) Results of Hoechst 33342 staining of chondrocytes after IL-1β stimulation. (**C**) Quantitative results of quantitative polymerase chain reaction analysis of IL-6. (**D**) Protein blotting images of IL-6 and BCL-2. (**E**) Results of quantification of protein blotting of IL-6 and BCL-2. (**F**) Lectin blot images of LTL and AAL, and locations of differential bands. (n=3). *P < 0.05, **P < 0.01.

After Treatment with Small Molecule Inhibitors and Knockdown of the Fucosyltransferase Gene, the Level of Fucosylation Decreased, Along with Improvement in Chondrocyte Inflammation

To continue to explore the relationship between fucosylation and chondrocyte inflammation, we decided to intervene in cellular glycosylation. We selected a small molecule inhibitor of fucosylation: 2-fluorofucose (SGN-2FF,2FF), which depletes the substrate of fucosylation: the GDP-fucose and inhibits fucosyltransferase activity. To prevent cytotoxicity, we determined the effect of different concentrations of SGN-2FF (1, 2, 5, 10, and 20 μM) at 12 (Figure 2A), 24 (Figure 2B) and 48 hours (Figure 2C), respectively, on the cell viability values of chondrocytes using the CCK8 assay; the results showed that the strongest values of cell viability were obtained at inhibitor concentrations of 2–5 μM (Supplementary Figure 1).

Subsequently, we divided the cells into four groups: normal chondrocytes (control group), cells after IL-1β treatment (OA group), cells treated with SGN-2FF (OA+2FF group), and cells treated with SGN-2FF only (2FF group) (all subgroups will be replaced by this abbreviation below). To verify whether chondrocyte inflammation was improved, we performed Calcein-AM /PI staining and cellular mitochondrial membrane potential JC-1 staining. Calcein-AM (calcineurin) emits a strong green fluorescence when bound to intracellular calcium ions, while PI (propidium iodide) stains only dead cells with disrupted cell membranes and produces red fluorescence. The staining results showed that the number of red fluorescence was less in the OA +2FF group compared with the OA group, indicating a decrease in the number of apoptotic cells (Figure 2D and E). Decrease in mitochondrial membrane potential is an important marker of early apoptosis; in normal cells with high mitochondrial membrane potential, JC-1 aggregated in the mitochondrial matrix and showed red fluorescence; conversely, JC-1 existed in the cytoplasm as a monomer and showed green fluorescence. We found that compared with the OA group, the intensity of red fluorescence was

https://doi.org/10.2147/JIR.S520179

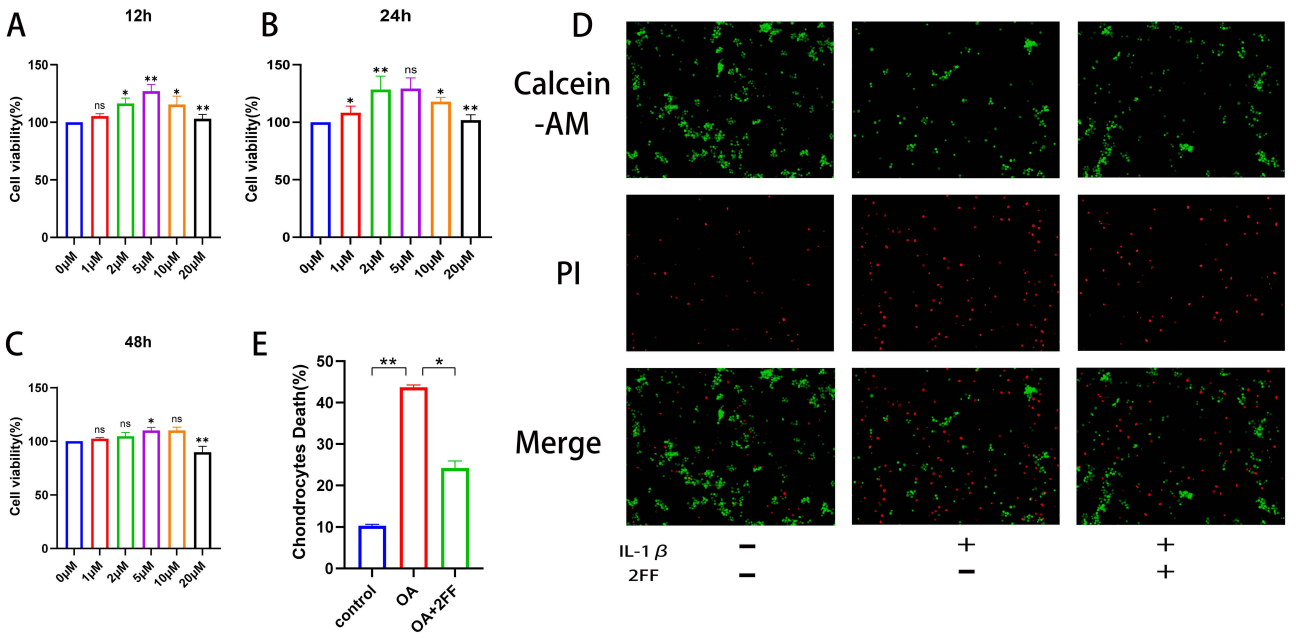

Figure 2 (**A**) After stimulation of cells with SGN-2FF, cell viability values were detected by CCK8 assay after 12 hours. (**B**) After stimulation of cells with SGN-2FF, cell viability values were detected by CCK8 assay after 24 hours. (**C**) After stimulation of cells with SGN-2FF, cell viability values were detected by CCK8 assay after 48 hours. (**D**) Calcein-AM/PI staining results after stimulation of chondrocytes using IL-1β and SGN-2FF. (**E**) Fluorescence quantitative analysis of chondrocyte mortality after stimulation of chondrocytes using IL-1β and SGN-2FF. (n=3). *P < 0.05, **P < 0.01.

higher and the intensity of green fluorescence decreased in the OA+2FF group, indicating that inhibition of fucosylation can effectively increase the mitochondrial membrane potential and improve mitochondrial function. (Figure 3A and B).

We did flow cytometry on the control group (Figure 3C), OA group (Figure 3D) and OA+2FF group (Figure 3E), respectively. Flow cytometry can identify different cell types of cell populations in the samples. The results showed that the number of apoptotic cells was significantly higher in the OA group, which indicated that IL1-β induced apoptosis, while inhibition of chondrocyte fucosylation reduced its apoptotic rate.

Meanwhile, we did lectin blotting for all four groups of cells. The results showed that compared with the OA group, the gray value of multiple bands shown in the OA+2FF group decreased; compared with the control group, the gray value of bands in the 2FF group was lower. This indicated that SGN-2FF indeed reduced the activation of fucose and inhibited the fucosylation of cells (Figure 4A and B).

In order to further validate that the inhibition of fucosylation led to the improvement of inflammation, we selected the key enzyme mediating fucosylation, namely fucosyltransferase 1 (FUT1), as the target of our study. It was hoped that knockdown of FUT1 would lead to the blockage of cellular fucosylation and its effect on chondrocyte inflammation would be observed. Thus, we designed siRNA against FUT1 and introduced this RNA into normal chondrocytes and chondroinflammatory cells for control experiments, respectively, by cell transfection technique. Based on the fluorescence indication, it was obvious that this siRNA was successfully introduced into the cell interior (Figure 4C). For the transfected cells, we extracted their RNA, and by quantitative polymerase chain reaction technique, we could find that the FUT1 gene was obviously down-regulated (Figure 4D). Meanwhile, Western blot also showed that FUT1 expression was down-regulated (Figure 4E and F). The expression of some target genes related to inflammation (IL-6, MMP-13) also showed a downward trend (Figure 4G–I).

From this we can basically conclude that it is entirely feasible to treat OA at the cellular level by alleviating chondrocyte inflammation by inhibiting inflammatory glycosylation.

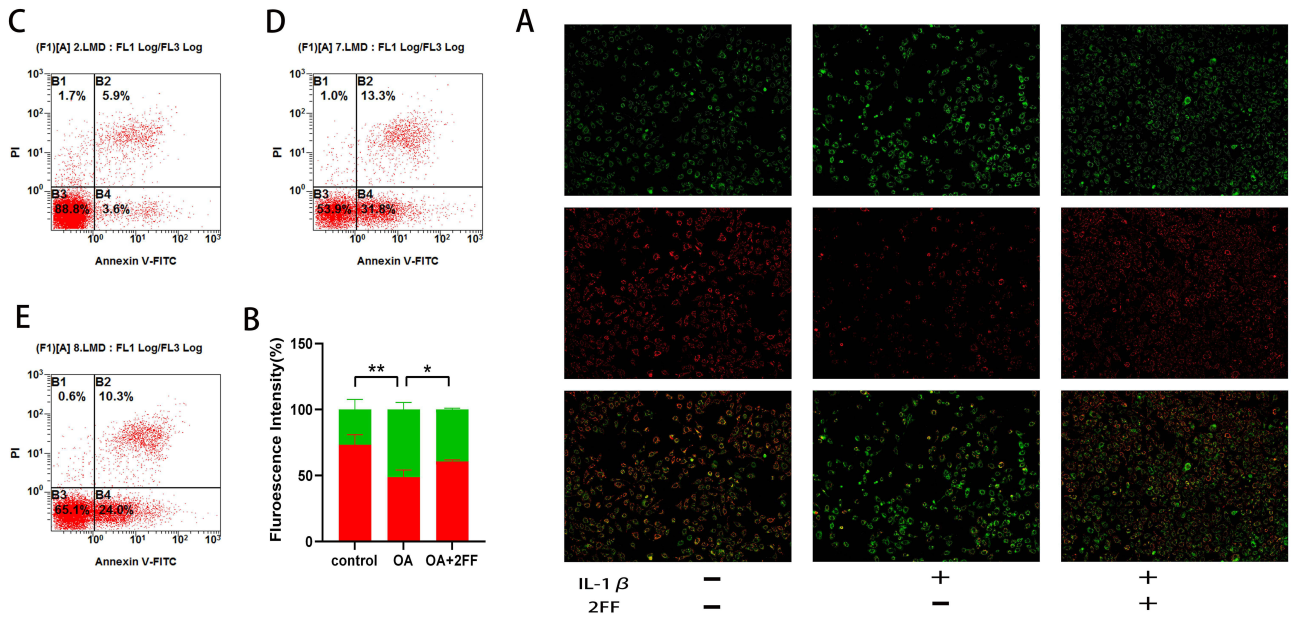

Figure 3 (**A**) JC-1 staining results of chondrocytes, with red fluorescence for healthy mitochondria and green fluorescence indicating mitochondrial dysfunction. (**B**) Quantitative fluorescence analysis of JC-1 staining. (**C**) Flow cytometry of control group for apoptosis detection results. (**D**) Flow cytometry of OA group for apoptosis detection results. (**E**) Flow cytometry of OA+2FF group for apoptosis detection results. (n=3). *P < 0.05, **P < 0.01.

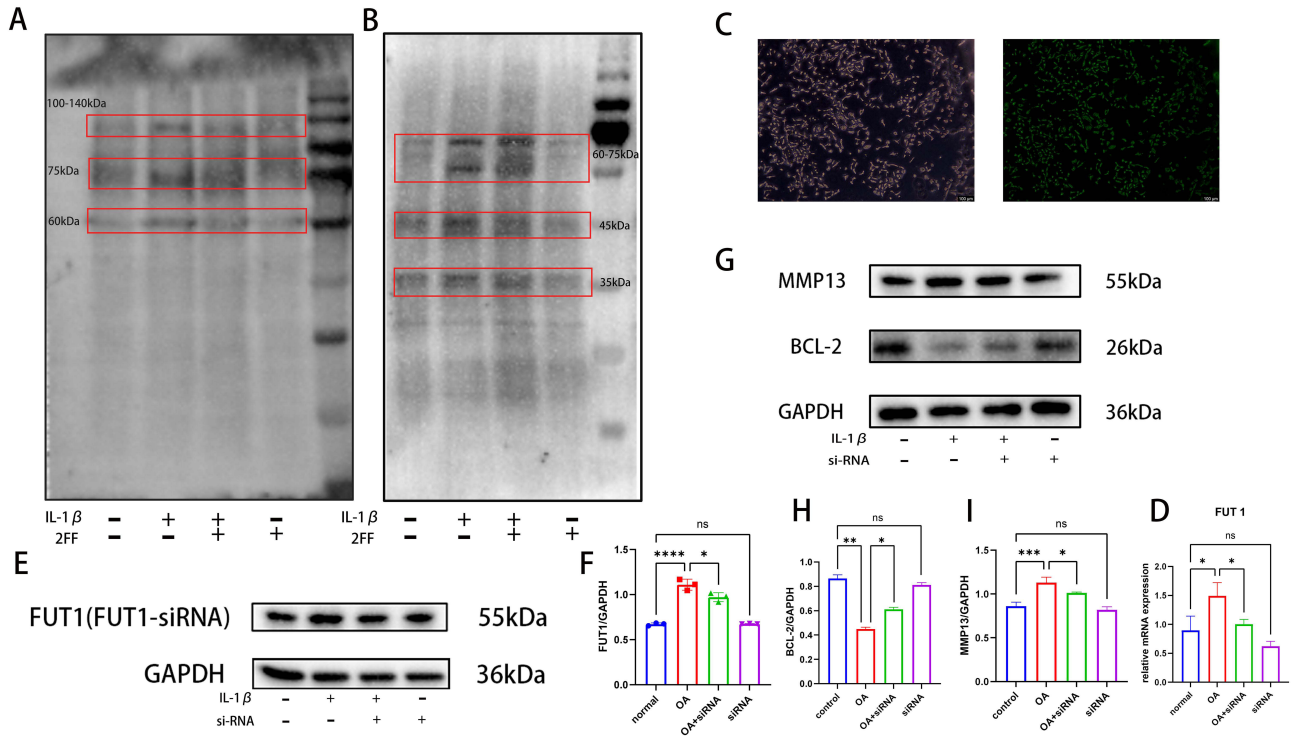

Figure 4 (**A**) Lectin blotting images of AAL, the and the positions of the differential bands. (**B**) Lectin blotting images of LTL, the and the positions of the differential bands. (**C**) Fluorescence images of FUT1-siRNA transfected chondrocytes, negative control. (**D**) Quantitative results of quantitative polymerase chain reaction of FUT1. (**E**) Protein blotting images of FUT1. (**F**) Quantitative results of protein blotting of FUT1. (**G**) Protein blotting images of MMP-13 and BCL-2. (**H**) Protein blotting quantification results of BCL-2. (**I**) Protein blotting quantification results of MMP-13. (n=3). *p < 0.05, **p < 0.01,***p < 0.001, ****p< 0.0001.

https://doi.org/10.2147/JIR.S520179

Upon Inhibition of Fucosylation, Activation of the Notch Pathway Is Suppressed, and Cellular Inflammatory Responses as Well as Extracellular Matrix Degradation are Ameliorated

Subsequently, we explored the mechanism by which rockweed glycosylation affects OA. We extracted RNA from cells in the control group, OA group, and OA+2FF group, respectively, and processed them for reverse transcription. Using quantitative polymerase chain reaction technology, the strength of gene expression of Notch1, JAG1, RBPJ and other iconic targets of the Notch pathway were examined respectively, and the results showed that the expression of Notch1, RBPJ and other genes were up-regulated compared with that of normal chondrocytes at the time of inflammation, and the expression of these genes was decreased after 2FF treatment (Figure 5D–G). This suggests that inhibition of fucosylation can affect the activation of the Notch pathway.

To further validate this finding, we subjected four groups of cells (same as 3.2) to immunofluorescence staining. We selected BCL-2 and NICD indicators for immunofluorescence double staining detection. BCL-2 controls the permeability of the mitochondrial membrane to regulate cell death, and is often used as a detection marker for apoptosis, and cleaved Notch1 (NICD) is the activated form of Notch1 obtained by shearing, which directly affects the expression of its downstream pathway. We stained these two indicators in the same cells, which can observe the apoptosis and Notch pathway activity at the same time. The results showed that the BCL-2 fluorescence intensity was significantly decreased in the OA group compared with the control group and the OA+2FF group, while the NICD fluorescence intensity was stronger; the NICD fluorescence intensity was lower than that in the control group in the 2FF group (Figure 5A–C). This indicates that inhibition of protein fucosylation can block the Notch pathway to a certain extent, while improving chondrocyte apoptosis and alleviating OA.

In addition, we detected the expression levels of Notch pathway-related proteins and inflammation-related proteins in the cells of the four groups by Western blot experiments. The results showed that the expression of Notch pathway proteins, such as Notch1, JAG1, and RBPJ, was significantly higher in the OA group than in the control group and the

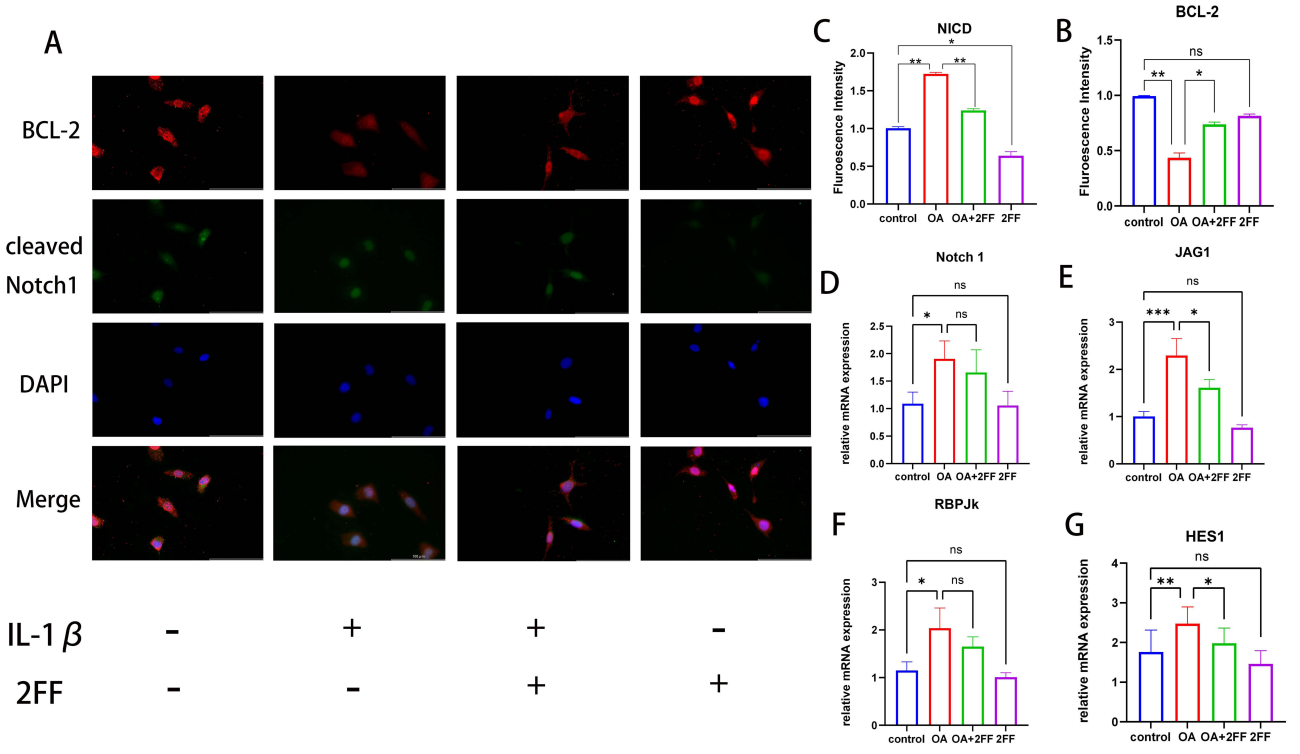

Figure 5 (**A**) Effect of inhibition of fucosylation on IL-1β-induced BCL-2 and NICD in the same chondrocytes, results of cellular immunofluorescence images. (**B** and **C**) Results of quantitative analysis of fluorescence intensity of BCL-2 and NICD. (**D**–**G**) Results of quantitative analysis of quantitative polymerase chain reaction of Notch1, JAG1, RBPJK and HES1. (n=3). *p < 0.05, **p < 0.01,***p < 0.001.

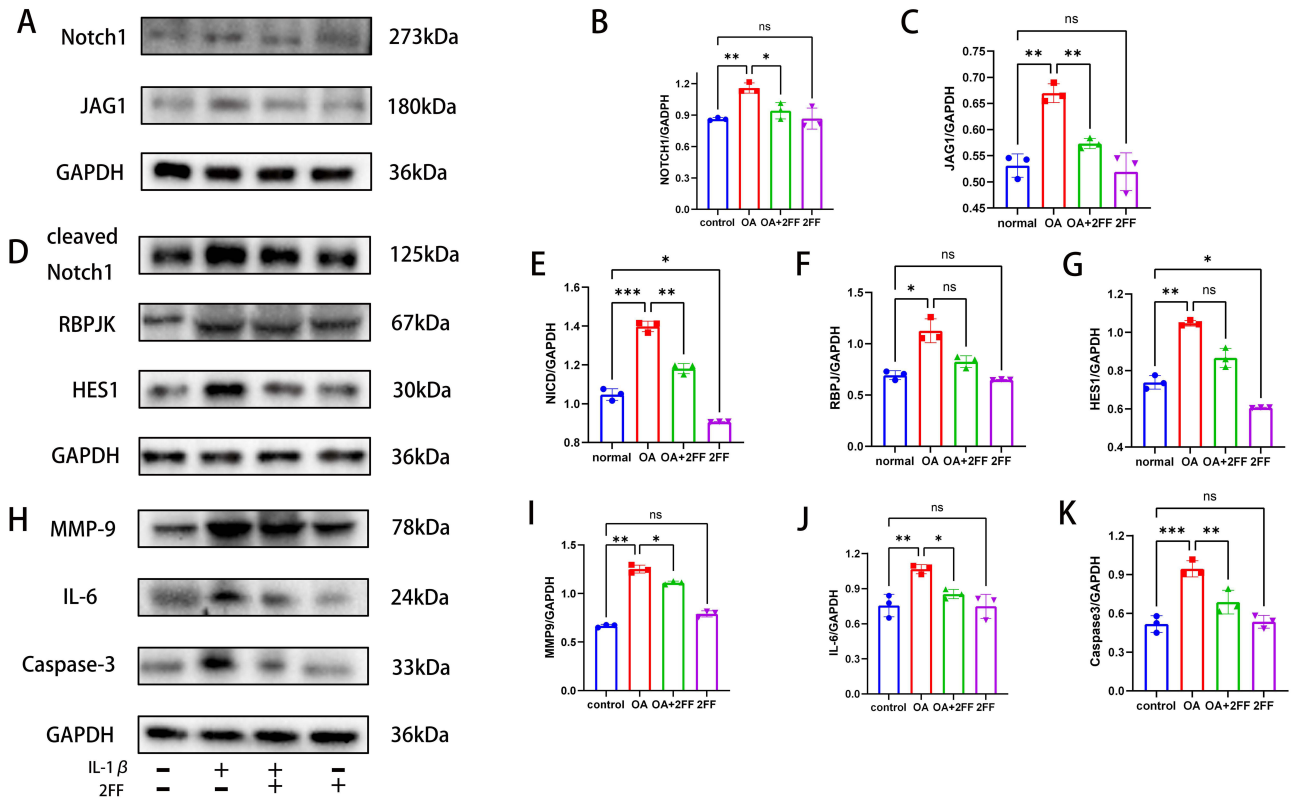

Figure 6 (**A**–**C**) Protein blotting images and quantitative results of Nocth1 and JAG1. (**D**–**G**) Protein blotting images and quantitative results of NICD, RBPJK and HES1. (**H**–**K**) Protein blotting images and quantitative results of MMP-9, IL-6 and Caspase-3. (n=3). *p < 0.05, **p < 0.01,***p < 0.001.

OA+2FF group. The expression of inflammation-related proteins such as MMP-9, IL-6, and Caspase-3[17] in the treated OA+2FF group showed significant downregulation compared to the OA group. The expression of NICD protein in the 2FF group showed significant downregulation compared to the control group; while the expression of RBPJ and HES1 was slightly downregulated (Figure 6). The above results were basically the same as the quantitative polymerase chain reaction results, which indicated that the inhibition of fucosylation of chondrocytes could inhibit the activity of Notch to a certain extent, thus reducing the production of inflammatory factors and achieving the purpose of alleviating chondrocyte inflammation.

The Condition of Surgically Modeled OA Rats was Improved by SGN-2FF Treatment

In order to clarify more clearly whether inhibition of fucosylation can delay OA, we designed in vivo experiments based on previous experiments. We surgically dissected the anterior cruciate ligament (ACL) and the medial meniscus of rats, causing the articular cartilage to rub against each other, leading to the development of OA. Based on the in vitro experiments, we divided the original treatment group (OA+2FF group) into a low-dose group (LOW) and a high-dose group (HIGH), and intervened using 2μM and 5μM concentrations of SGN-2FF, respectively. Subsequently, we similarly divided the rats into four groups (denoted by control group, OA group, OA+2FF group LOW and OA+2FF group HIGH, respectively). The treatment group was administered to the rats by means of 50ul of drug injected into the joint cavity. The joint cavity injection was performed every 3 days, and the treatment cycle was 11–14 weeks, and their knee joints and serum samples were obtained for analysis and testing.

We performed ELISA on the extracted serum to detect TNF-α and IL-6 indexes in the serum of rats at week 12. The standard curve was plotted according to the concentration of standards (R2=0.9751). It was found that the expression of TNF-α and IL-6 in rats in the OA group was significantly higher than that in the other three groups, and the decreasing trend was obvious in the high-dose group (Figure 7C).

https://doi.org/10.2147/JIR.S520179

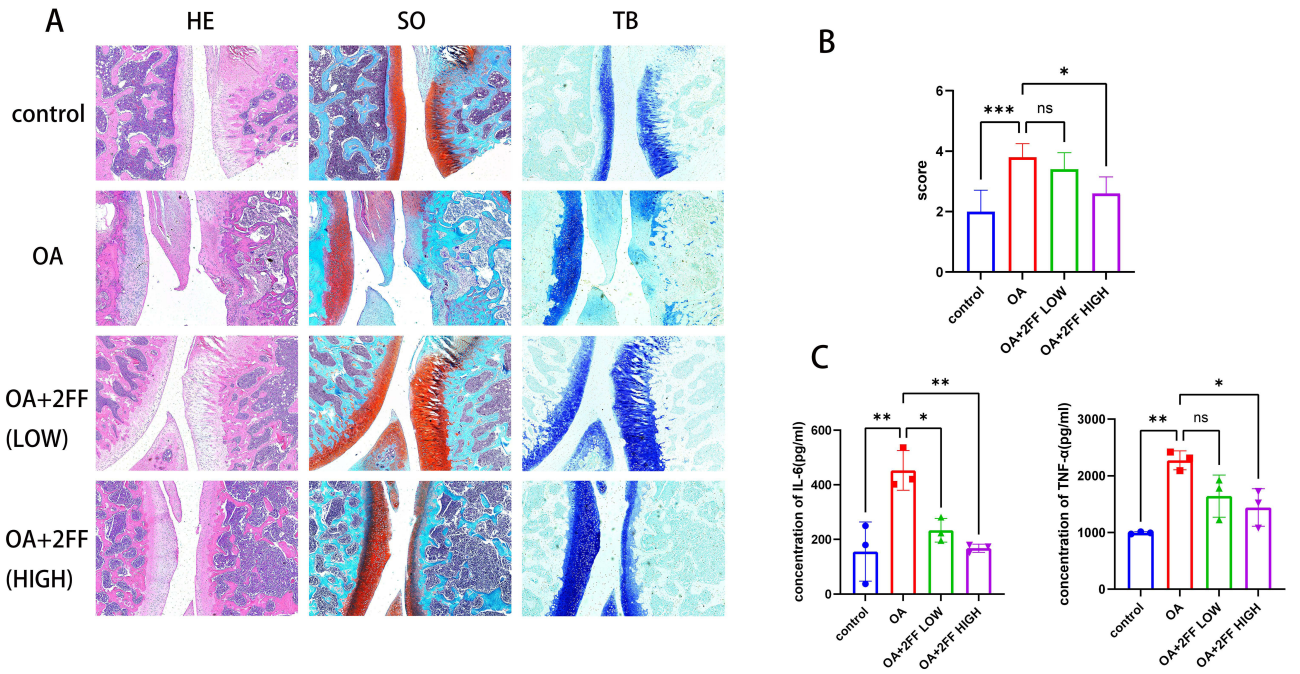

Figure 7 (**A**) HE, SO and TB staining results of rat knee cartilage from different experimental groupings (control, OA, OA+2FF LOW, OA+2FF HIGH groups) (Concentration 2μM/5μM). (**B**) OARSI scores of cartilage in different experimental groups. (**C**) Expression levels of TNF-α and IL-6 in rat serum, quantitative analysis of ELISA results. (n=3). *P < 0.05, **P < 0.01,***P < 0.001.

We did decalcification of the obtained knee joint samples, made paraffin sections and stained them with HE, SO and TB staining, so as to observe the effect of drug treatment. The results showed that in the OA group, the knee cartilage was severely damaged, the number of chondrocytes was reduced and disordered, the surface was rough, and the level of proteoglycan was low; in contrast, the cartilage in the OA+2FF group had been repaired to a certain extent, the number of chondrocytes was increased and aligned, the surface of the cartilage was more smooth, and the level of proteoglycan was restored. There was little overall difference between the high-dose and low-dose groups (Figure 7A). To further assess the extent of cartilage damage, we used the Osteoarthritis Research Society International (OARSI) scoring criteria, which combines changes in cartilage structure, cell number, and matrix quality. Higher scores indicate more severe cartilage damage. The results showed that the OARSI score in the OA group was significantly higher than that in the control group, which was reduced after SGN-2FF intervention (Figure 7B).

Considering that OA also affects bone morphology and leads to joint deformation. We did Micro-CT test on four groups of joint samples, this test can visualize the bone density, strength and integrity, as well as bone proliferation and destruction, and the formation of bone redundancy. We utilized this technique to perform imaging and 3D reconstruction of bone for the four groups of samples and calculated parameters such as bone volume ratio (BV/TV), (Figure 8E) trabecular thickness (Tb. Th), (Figure 8F) trabecular number (Tb. N) (Figure 8G), and trabecular space (Tb. Sp) (Figure 8H). Imaging showed a certain degree of hyperplasia and destruction of the knee joint in the OA group, which caused the formation of bone capillaries and increased bone resorption; whereas these symptoms were improved to a certain extent in the treatment group. (Figure 8A–D) In addition, compared with the OA group, rats in the high-dose group showed significant increases in BV/TV, Tb. Th, and Tb. N, and a decrease in Tb. Sp levels. Such results indicate that the injection of fucosylation inhibitor through the joint cavity can significantly improve the joint damage and inhibit the changes of bone morphology in rats, which is beneficial for the treatment of OA.

Discussions

OA is a degenerative joint disease characterized by degenerative changes in articular cartilage and secondary osteophytes, which can lead to joint pain, stiffness, and even deformity, seriously affecting patients' quality of life.[18] Although

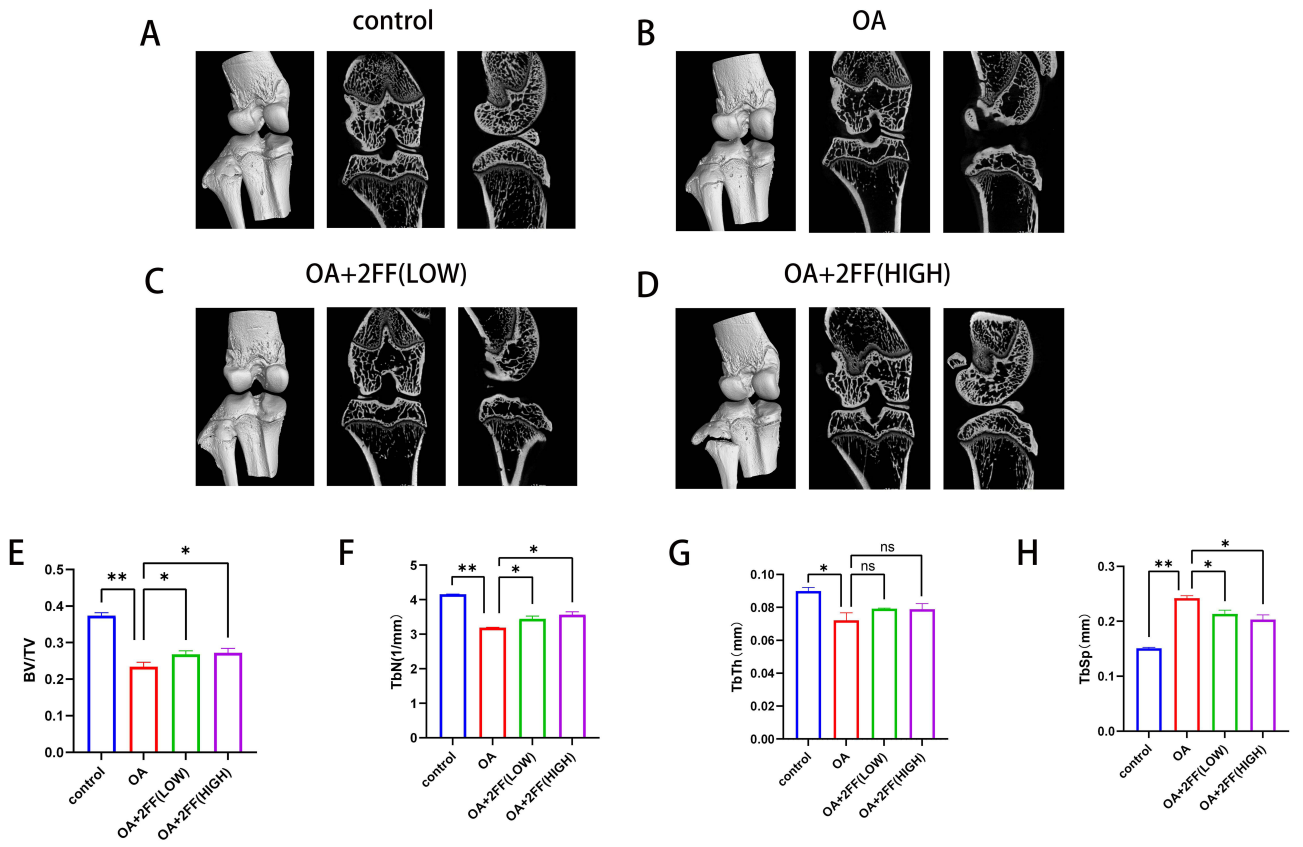

Figure 8 (**A**–**D**) Typical images of 3D reconstructed, sagittal and coronal surfaces of rat knee joints in different experimental groupings (control, OA, OA+2FF LOW, OA +2FF HIGH groups). (**E**–**H**) Quantitative analysis of BV/TV, Tb.N, Tb.Sp, and Tb.Th results of rat knee joints in different experimental groupings. (n=3). *P < 0.05, **P < 0.01.

the pathogenesis of OA is complex, lesions of articular cartilage are the most important. Damage to cartilage leads to gradual wear and deformation of the joints during frequent activities, and the lack of blood vessels, lymphatic vessels, and nerve fibers in cartilage tissues makes it difficult to repair the damage; whereas apoptosis and degradation of chondrocytes severely affects their synthesis and secretion functions and interferes with extracellular matrix metabolism, while leading to activation of MMPs, the and elevated levels of pro-inflammatory cytokines such as TNF-α, IL-1β and IL-6, aggravating the process of OA.[19–21] Abnormalities in glycan structure occur in a variety of diseases, and abnormal protein glycosylation is likewise an important factor in the development of OA. In the present experiments, we observed an abnormal elevation of fucosylation in OA cartilage, and it has been reported that altered glycosylation plays an important role in the degenerative changes of chondrocytes and contributes to the onset and progression of OA.[12] Inhibition of fucosylation modulates protein translation of catabolic enzymes in human myeloid cells in response to inflammation.[22,23] In response to this phenomenon, we inhibited fucosylation of chondrocytes by pharmacological intervention. It was shown that inhibition of fucosylation resulted in a significant decrease in chondrocyte apoptosis and down-regulation of the expression of metalloproteinases (MMP-9, MMP-13). These metalloproteinases have the ability to cleave type II collagen and are involved in cartilage degradation.[24] For further validation, we down-regulated the key enzyme of fucosylation, ie, fucosyltransferase 1, by si-RNA, and the results showed that fucosylation decreased and OA cartilage was alleviated. Of course, we noticed that the effect of achieving inhibition of fucosylation by inhibiting FUT1 was not particularly obvious. This may be due to the fact that there is more than one type of transferase involved in this process, and some enzymes related to the synthesis of cartilage matrix components also play an important role; fucosyltransferase 2 (FUT2) also adds α-1,2-fucose, but it is mainly responsible for the fucosylation of secretory glycoproteins.[25]

https://doi.org/10.2147/JIR.S520179

The Notch pathway is an ancient and highly conserved pathway that is closely related to catabolism and synthesis during cartilage ECM development. The Notch signaling pathway consists of Notch receptors (Notch1-4), Notch ligands (DLL1, DLL3, DLL4, JAG1, and JAG2), DNA-binding proteins such as the CSL (CBF-1, suppressor of hairless, Lag), and other effectors and Notch regulatory molecules of hairless, Lag) DNA-binding proteins, and other effectors and regulatory molecules of Notch, among other components.[26] The signal is generated by the interaction and binding of receptors and ligands between neighboring cells, which causes conformational changes in the Notch receptor, then undergoes a series of complex shearing processes (with the participation of metalloproteinase converting enzyme, γ-secretase, etc), and ultimately obtains the Notch receptor intracellular structural domain (NICD) and releases it from the membrane, and the NICD then enters the nucleus, binds to the transcription factor RBPJ, activating the transcription of downstream genes.[27] The downstream classical targets of the notch pathway include Hes1, Hes3, Hes5, etc. and Hey1, Hey2, etc,[28] which in turn can be linked to other pathways, eg, it has been found that Hes1 can activate the catabolic factors Adams5, Mmp13, and IL6, etc, with the help of certain cofactors (eg, calcium/calmodulin-dependent protein kinase 2δ (CaMK2δ)), to induce chondrocyte breakdown, IL6, etc, inducing chondrocyte catabolism and participating in the pathogenesis of OA.[29] In addition the notch pathway is also indirectly linked to the nuclear factor activator-κB (NF-κB) and tumor growth factor-β (TGF-β) pathways, which are the classical pathways contributing to the development of inflammation.[26] Therefore, notch pathway not only regulates cartilage development and maintains homeostasis, but also participates in the development of osteoarthritis. w.F. WANG et al investigated the effect of microRNA (miR-145) on apoptosis of OA chondrocytes, and found that miR-145 was under-expressed in OA chondrocytes and notch was usually over-activated; whereas, the notch pathway in miR-145 mimic group was over-expressed in OA chondrocytes, and the notch pathway in the notch pathway in the notch pathway in the notch pathway mimics group. mimic group the notch pathway was inhibited and OA was alleviated.[30] Another study found that notch molecules showed high expression in temporomandibular osteoarthritis, and the researchers induced OA by surgery and examined the expression of notch pathway markers Notch1, JAG1 and Hes1, which they found were activated at the onset of OA and increased significantly over time.[31]

There are a large number of EGF repeats in the Notch1 receptor, and FUT1 adds O-conjugated fucose to the folded EGF repeats containing the shared sequence C2-X-X-X-X-X-(S/T)-C3, after which Fringe adds subsequent glycans (LFMG, MFNG, RFNG) on top of the O-fucose.[32,33] This process occurs in the endoplasmic reticulum and Golgi apparatus, and is related to whether Notch1 has a normal function, and is the key to Notch1 being able to bind to ligands such as JAG1.[34] Inhibition of fucosylation, on the other hand, prevents this process from taking place, which down-regulates the activity of the Notch pathway, resulting in a decrease in downstream HES1 expression, thereby inhibiting the production of inflammatory factors such as Mmp13 and IL-6. In our experiments, we found that the expression of Notch1 and JAG1 in normal cartilage hardly changed after inhibition of fucosylation. This is due to the fact that glycosylation relates to the correct folding of Notch1 and affects its normal function, but does not have an effect on how much Notch1 is present; JAG1, as a ligand, will not be affected by the dysfunction of Notch1. However, in OA, we noticed a decrease in the expression of Notch1 and JAG1, which we deduced to be due to the inflammatory state that resulted in abnormally elevated activation of the Notch pathway, and the inhibition of fucosylation that resulted in improvement of cartilage inflammation and extracellular matrix degradation, which resulted in a decrease in the activation of the Notch pathway. Similarly, the same trend was observed for the downstream key target, RBPJ. The Notch pathway is different from other inflammatory pathways in that it lacks traditional phosphorylation targets, and the completion of S2 and S3 shearing of the Notch receptor is generally regarded as a marker of phosphorylation activation. The NICD obtained by shearing, as the intracellular structural domain of Notch receptor, can enter the downstream pathway of nucleus radicalization, which is the key to whether the Notch pathway can be conducted downward, and is also regarded as the active component of Notch. Unlike Notch1, NICD expression showed a significant downward trend with either SGN-2FF or FUT1-si-RNA intervention in chondrocytes, suggesting that inhibition of fucosylation can indeed be achieved to modulate the Notch pathway. HES1 also showed the same trend as NICD. After control experiments, we found that as the activation of Notch pathway decreased, the expression of bcl-2 appeared to be elevated, while the expression of caspase-3, MMP-13, IL-6, etc. decreased. After analyzing ELISA experiments on animal samples, we obtained the same conclusion. Therefore, we have reason to believe that inhibition of fucosylation

can ameliorate chondrocyte apoptosis and matrix degradation by decreasing the production of the active components of the Notch receptor, thereby blocking the Notch pathway and decreasing the secretion of pro-inflammatory factors and metalloproteinases.

Of course, there are numerous pathogenic mechanisms of OA, similar to the Notch pathway, the NF-κB pathway, the TGF-β1 pathway, and so on. These pathways are inextricably linked to the Notch pathway. Firstly, the Notch pathway has much in common with the NF-κB pathway, and both can not only play a role in cellular value-addition, differentiation and apoptosis, but can also be activated by factors such as TNF-α and ischaemia-hypoxia.[35] In addition to this, there are many examples that validate the interaction of the Notch pathway with the NF-κB pathway. T Palaga et al[36] found that inhibition of Notch receptor activation significantly reduced proliferation in CD4 and CD8 T cells and blocked NF-κB pathway activity and IFN-γ production in peripheral T cells. Blocking Notch pathway activation in mice also significantly downregulated NF-κB expression. When the Notch pathway was blocked with DAPT inhibitors, phosphorylation of IκB kinase (IKK) α/β as well as IκB-α was inhibited and NF-κB pathway activity decreased.[37] These suggest that the Notch pathway can regulate the activity of the NF-κB pathway to some extent. Notably, the increased expression level of p65-NF-κB protein greatly enhanced the Notch-mediated activation of the Hes1 promoter. NF-κB can also regulate the SMRT/N-COR transcriptional corepressor, deregulate the repressive effect of the SMRT/N-COR complex on the target gene, and increase the activation of HES1.[38] The study by F Oakley et al[39] showed that overexpression of RBPJκ in the Notch pathway in hepatic stellate cells (HSCs) significantly reduced the expression of core inhibitory protein IκBα and increased NF-κB DNA binding activity; The expression of IkBa can be inhibited by NICD, which recruits histone acetylases to convert RBPJκ into transcriptional activators. These studies have shown that increased activation of Notch expression increases NF-κB activity, whereas inhibition of Notch leads to a decrease in NF-κB activity, and that the two pathways can mutually regulate each other with the help of various components of the transduction pathway, and that their dysregulation is a common feature in the development of inflammation. In addition, the Notch pathway can interact with other pathways. The cytokine interleukin 22 (IL-22) or the Notch pathway inhibitor dibenzazepine (DBZ) can ameliorate inflammation induced by TGF-β1 while downregulating the Notch pathway.[40] The down-regulation of pro-inflammatory factors such as IL-6 and TNF-α in response to decreased Notch1 activity, which we detected by Western blotting and ELISE, is partly due to the combined effects of these non-classical pathways. In addition, activation of the Notch pathway can also affect macrophage polarization, and it has been shown that Notch1, JAG1, and Hes1 all appear upregulated in addition to an increase in the CD86/CD206 ratio when polarization is induced in M1 macrophages. We believe that this is partly due to the fact that the inhibition of fucosylation using SGN-2FF reduces Notch pathway activity, which hinders the polarization of M1 cells and reduces the release of matrix metalloproteinases (MMPs), thus reducing the breakdown of cartilage matrix and chondrocyte destruction.[41]

OA is a comprehensive disease that is not only reflected in cartilage lesions, but also accumulates lesions in bone, subchondral bone, and synovium.[42] In animal experiments, we examined the indicators of OA in bone and subchondral bone. The imaging results showed that after the injection of fucosylation inhibitor through the joint cavity, the bone density and strength around the knee joint of rats were improved compared with that of the OA group, and the joint space became smaller, and the cartilage was aligned more neatly with fewer defects. This suggests that inhibition of fucosylation can have a favorable effect not only on chondrocytes but also on knee OA. Fucosylation is a common chemical reaction in mammalian cells, and this process is accomplished by assembling the fucose in guanosine diphosphate (GDP)-fucose to the end of the proteoglycan side chain by fucosyltransferases.[43] In order to reduce the level of fucosylation, the inhibitor SGN-2FF we used is a small molecule preparation that has passed Phase I clinical trials. It can be converted into the active ingredient GDP-2-fluorofucose (GDP-2FF) after entering cells, and can inhibit intracellular glycosylation by depleting the substrate GDP fucose and inhibiting various fucosyltransferases. In preclinical experiments, this drug demonstrated excellent antitumor activity within a mouse model and was well tolerated, with no significant acute toxicity events reported. SGN-2FF also showed anti-inflammatory properties, and in response to acetaminophen-induced acute hepatic injury, 2FF significantly inhibited oxidative stress and mitochondrial damage and reduced the expression of inflammation-related proteins.[44] However, in the course of continued dose increases, 2FF has also been exposed to a number of side effects, the most common being diarrhea, exertion, and nausea. However, it is alarming to note that thromboembolism has been observed in clinically treated patients, which may be related to the

role of fucosylation in leukocyte adhesion, despite studies suggesting that 2FF may be beneficial in preventing or treating the vaso-occlusive condition of sickle cell disease (SCD).[45]

Conclusion

Our study shows that fucosylation is abnormally elevated in OA cartilage and chondrocytes. In addition, by silencing FUT1 and the small molecule inhibitor SGN-2FF both can inhibit the level of fucosylation to a certain extent, interfering with the normal folding of the Notch1 receptor and decreasing the expression of its activated form, NICD, thus affecting the signaling of the Notch pathway, impeding the production of inflammatory factors, such as IL-6, TNF-α, and delaying chondrocyte senescence and apoptosis. Our work verified the therapeutic effect of inhibition of fucosylation on chondrocyte inflammation and elucidated part of its mechanism of action through in vitro as well as in vivo experiments, further confirming the anti-inflammatory and antioxidant effects of inhibition of fucosylation and filling the gap of mechanistic studies of glycomics in bone and joint diseases. Although the in vivo study lacked the comparison with the efficacy of other anti-inflammatory drugs, it is undeniable that the treatment against OA fucosylation is practicable, which provides a reference for the research of clinical drugs and a new idea for the treatment of OA.

Data Sharing Statement

The data presented in this study are available in the article.

Institutional Review Board Statement

Experiments involving animals have been approved by the Animal Ethics Committee of Xi'an Jiaotong University. (XJTUAE2023-1640) The animal welfare guidelines for this experiment are the GB/T35892-2018 Ethical Review Guidelines for Laboratory Animal Welfare at Xi'an Jiaotong University.

Funding

This study was supported by the General Project (Social Development Field) of the Science and Technology Department of Shaanxi Province (Grant No. 2023-YBSF-488), Xi'an Health Bureau Scientifc Research Project (Grant No. 2023ms15).

Disclosure

The authors declare that there is no conflict of interest in this work.

References

1. Hunter DJ, Bierma-Zeinstra S. Osteoarthritis. *Lancet*. 2019;393(10182):1745–1759. PMID: 31034380. doi:10.1016/S0140-6736(19)30417-9
2. Magalhães A, Duarte HO, Reis CA. The role of O-glycosylation in human disease. *Mol Aspects Med*. 2021;79:100964. PMID: 33775405. doi:10.1016/j.mam.2021.100964
3. Naito K, Takahashi M, Kushida K, et al. Measurement of matrix metalloproteinases (MMPs) and tissue inhibitor of metalloproteinases-1 (TIMP-1) in patients with knee osteoarthritis: comparison with generalized osteoarthritis. *Rheumatology*. 1999;38(6):510–515. PMID: 10402070. doi:10.1093/rheumatology/38.6.510
4. Zhang HB, Zhang Y, Chen C, Li YQ, Ma C, Wang ZJ. Pioglitazone inhibits advanced glycation end product-induced matrix metalloproteinases and apoptosis by suppressing the activation of MAPK and NF-κB. *Apoptosis*. 2016;21(10):1082–1093. PMID: 27515513. doi:10.1007/s10495-016-1280-z
5. Dall'Olio F, Vanhooren V, Chen CC, Slagboom PE, Wuhrer M, Franceschi C. N-glycomic biomarkers of biological aging and longevity: a link with inflammaging. *Ageing Res Rev*. 2013;12(2):685–698. PMID: 22353383. doi:10.1016/j.arr.2012.02.002
6. Onu I, Gherghel R, Nacu I, et al. Can combining hyaluronic acid and physiotherapy in knee osteoarthritis improve the physicochemical properties of synovial fluid? *Biomedicines*. 2024;12(2):449. PMID: 38398051; PMCID: PMC10886650. doi:10.3390/biomedicines12020449
7. Sherman SL, Thyssen E, Nuelle CW. Osteochondral autologous transplantation. *Clin Sports Med*. 2017;36(3):489–500. doi:10.1016/j.csm.2017.02.006
8. Gherghel R, Onu I, Iordan DA, et al. A new approach to postoperative rehabilitation following mosaicplasty and Bone Marrow Aspiration Concentrate (BMAC) augmentation. *Biomedicines*. 2024;12(6):1164. PMID: 38927371; PMCID: PMC11200487. doi:10.3390/biomedicines12061164
9. Frehner F, Benthien JP. Microfracture: state of the Art in Cartilage Surgery[J]? *Cartilage*. 2018;9(4):339–345. doi:10.1177/1947603517700956
10. Fujita K, Hatano K, Hashimoto M, et al. Fucosylation in urological cancers. *Int J Mol Sci*. 2021;22(24):13333. PMID: 34948129; PMCID: PMC8708646. doi:10.3390/ijms222413333

11. Ma B, Simala-Grant JL, Taylor DE. Fucosylation in prokaryotes and eukaryotes. *Glycobiology*. 2006;16(12):158R–84R. doi:10.1093/glycob/cwl040
12. Tardio L, Andrés-Bergós J, Zachara NE, et al. O-linked N-acetylglucosamine (O-GlcNAc) protein modification is increased in the cartilage of patients with knee osteoarthritis. *Osteoarthritis Cartilage*. 2014;22(2):259–263. PMID: 24333294. doi:10.1016/j.joca.2013.12.001
13. Yu H, Li M, Wen X, et al. Elevation of α-1,3 fucosylation promotes the binding ability of TNFR1 to TNF-α and contributes to osteoarthritic cartilage destruction and apoptosis. *Arthritis Res Ther*. 2022;24(1):93. PMID:35488351; PMCID: PMC9052622. doi:10.1186/s13075-022-02776-z
14. Schneider M, Al-Shareffi E, Haltiwanger RS. Biological functions of fucose in mammals. *Glycobiology*. 2017;27:601–618. [PubMed: 28430973]. doi:10.1093/glycob/cwx034
15. Varshney S, Stanley P. Multiple Roles for O-Glycans in Notch Signalling. *FEBS Lett*. 2018;592:3819–3834. Excellent, recent comprehensive review of O-glycans occuring on the Notch receptor [PubMed: 30207383]. doi:10.1002/1873-3468.13251
16. Ashkenazi A, Fairbrother WJ, Leverson JD, Souers AJ. From basic apoptosis discoveries to advanced selective BCL-2 family inhibitors. *Nat Rev Drug Discov*. 2017;16(4):273–284. PMID: 28209992. doi:10.1038/nrd.2016.253
17. Asadi M, Taghizadeh S, Kaviani E, et al. Caspase-3: structure, function, and biotechnological aspects. *Biotechnol Appl Biochem*. 2022;69(4):1633–1645. PMID: 34342377. doi:10.1002/bab.2233
18. Glyn-Jones S, Palmer AJ, Agricola R, et al. Osteoarthritis. *Lancet*. 2015;386(9991):376–387. PMID: 25748615. doi:10.1016/S0140-6736(14)60802-3
19. Knights AJ, Redding SJ, Maerz T. Inflammation in osteoarthritis: the latest progress and ongoing challenges. *Curr Opin Rheumatol*. 2023;35(2):128–134. PMID: 36695054; PMCID: PMC10821795. doi:10.1097/BOR.0000000000000923
20. Kapoor M, Martel-Pelletier J, Lajeunesse D, Pelletier JP, Fahmi H. Role of proinfammatory cytokines in the pathophysiology of osteoarthritis. *Nat Rev Rheumatol*. 2011;7(1):33–42. doi:10.1038/nrrheum.2010.196
21. Wang P, Guan PP, Guo C, Zhu F, Konstantopoulos K, Wang ZY. Fluid shear stress-induced osteoarthritis: roles of cyclooxygenase-2 and its metabolic products in inducing the expression of proinfammatory cytokines and matrix metalloproteinases. *FASEB J*. 2013;27(12):4664–4677. doi:10.1096/fj.13-234542
22. Li J, Hsu HC, Mountz JD, Allen JG. Unmasking fucosylation: from cell adhesion to immune system regulation and diseases. *Cell Chem Biol*. 2018;25(5):499–512. doi:10.1016/j.chembiol.2018.02.005
23. Joyce K, Mohd Isa IL, Krouwels A, Creemers L, Devitt A, Pandit A. The role of altered glycosylation in human nucleus pulposus cells in infammation and degeneration. *Eur Cell Mater*. 2021;41:401–420. doi:10.22203/eCM.v041a26
24. Hu Q, Ecker M. Overview of MMP-13 as a Promising Target for the Treatment of Osteoarthritis. *Int J Mol Sci*. 2021;22(4):1742. PMID: 33572320; PMCID: PMC7916132. doi:10.3390/ijms22041742
25. Li J, Hsu HC, Ding Y, et al. Inhibition of fucosylation reshapes inflammatory macrophages and suppresses type II collagen-induced arthritis. *Arthritis Rheumatol*. 2014;66(9):2368–2379. PMID: 24838610; PMCID: PMC4146698. doi:10.1002/art.38711
26. Zhou B, Lin W, Long Y, et al. Notch signaling pathway: architecture, disease, and therapeutics. *Signal Transduct Target Ther*. 2022;7(1):95. PMID: 35332121; PMCID: PMC8948217. doi:10.1038/s41392-022-00934-y
27. Mumm JS, Schroeter EH, Saxena MT, et al. A ligand-induced extracellular cleavage regulates gamma-secretase-like proteolytic activation of Notch1. *Mol Cell*. 2000;5(2):197–206. PMID: 10882062. doi:10.1016/s1097-2765(00)80416-5
28. Artavanis-Tsakonas S, Rand MD, Lake RJ. Notch signaling: cell fate control and signal integration in development. *Science*. 1999;284(5415):770–776. PMID: 10221902. doi:10.1126/science.284.5415.770
29. Sugita S, Hosaka Y, Okada K, et al. Transcription factor Hes1 modulates osteoarthritis development in cooperation with calcium/calmodulin-dependent protein kinase 2. *Proc Natl Acad Sci U S A*. 2015;112(10):3080–3085. PMID: 25733872; PMCID: PMC4364241. doi:10.1073/pnas.1419699112
30. Wang WF, Liu SY, Qi ZF, Lv ZH, Ding HR, Zhou WJ. MiR-145 targeting BNIP3 reduces apoptosis of chondrocytes in osteoarthritis through Notch signaling pathway. *Eur Rev Med Pharmacol Sci*. 2020;24(16):8263–8272. PMID: 32894532. doi:10.26355/eurrev_202008_22622
31. Lan L, Jiang Y, Zhang W, Li T, Ying B, Zhu S. Expression of Notch signaling pathway during osteoarthritis in the temporomandibular joint. *J Craniomaxillofac Surg*. 2017;45(8):1338–1348. PMID: 28684076. doi:10.1016/j.jcms.2017.05.029
32. Kakuda S, Haltiwanger RS. Deciphering the fringe-mediated notch code: identification of activating and inhibiting sites allowing discrimination between ligands. *Dev Cell*. 2017;40(2):193–201. PMID: 28089369; PMCID: PMC5263050. doi:10.1016/j.devcel.2016.12.013
33. Wang Y, Lee GF, Kelley RF, Spellman MW. Identification of a GDP-L- fucose: polypeptide fucosyltransferase and enzymatic addition of O-linked fucose to EGF domains. *Glycobiology*. 1996;6(8):837–842. PMID: 9023546. doi:10.1093/glycob/6.8.837
34. Karlsson C, Lindahl A. Notch signaling in chondrogenesis. *Int Rev Cell Mol Biol*. 2009;275:65–88. PMID: 19491053. doi:10.1016/S1937-6448(09)75003-8
35. Ang HL, Tergaonkar V. Notch and NFkappaB signaling pathways: do they collaborate in normal vertebrate brain development and function? *Bioessays*. 2007;29(10):1039–1047. PMID: 17876798. doi:10.1002/bies.20647
36. Palaga T, Miele L, Golde TE, Osborne BA. TCR-mediated Notch signaling regulates proliferation and IFN-gamma production in peripheral T cells. *J Immunol*. 2003;171(6):3019–3024. PMID: 12960327. doi:10.4049/jimmunol.171.6.3019
37. Li L, Jin JH, Liu HY, et al. Notch1 signaling contributes to TLR4-triggered NF-κB activation in macrophages. *Pathol Res Pract*. 2022;234:153894. PMID: 35489123. doi:10.1016/j.prp.2022.153894
38. Espinosa L, Santos S, Inglés-Esteve J, Muñoz-Canoves P, Bigas A. p65-NFkappaB synergizes with Notch to activate transcription by triggering cytoplasmic translocation of the nuclear receptor corepressor N-CoR. *J Cell Sci*. 2002;115(Pt 6):1295–1303. PMID: 11884528. doi:10.1242/jcs.115.6.1295
39. Oakley F, Mann J, Ruddell RG, Pickford J, Weinmaster G, Mann DA. Basal expression of IkappaBalpha is controlled by the mammalian transcriptional repressor RBP-J (CBF1) and its activator Notch1. *J Biol Chem*. 2003;278(27):24359–24370. PMID: 12700242. doi:10.1074/jbc.M211051200
40. Tang R, Xiao X, Lu Y, et al. Interleukin-22 attenuates renal tubular cells inflammation and fibrosis induced by TGF-β1 through Notch1 signaling pathway. *Ren Fail*. 2020;42(1):381–390. PMID: 32338120; PMCID: PMC7241524. doi:10.1080/0886022X.2020.1753538
41. Hu X, Hong B, Shan X, et al. The Effect of *Poria cocos* Polysaccharide PCP-1C on M1 Macrophage Polarization via the Notch Signaling Pathway. *Molecules*. 2023;28(5):2140. PMID: 36903383; PMCID: PMC10004619. doi:10.3390/molecules28052140

42. Abramoff B, Caldera FE. Osteoarthritis: pathology, Diagnosis, and Treatment Options. *Med Clin North Am*. 2020;104(2):293–311. PMID: 32035570. doi:10.1016/j.mcna.2019.10.007
43. Becker DJ, Lowe JB. Fucose: biosynthesis and biological function in mammals. *Glycobiology*. 2003;13(7):41R–53R. PMID: 12651883. doi:10.1093/glycob/cwg054
44. Liu Z, Tu M, Shi J, et al. Inhibition of fucosylation by 2-fluorofucose attenuated Acetaminophen-induced liver injury via its anti-inflammation and anti-oxidative stress effects. *Front Pharmacol*. 2022;13:939317. PMID: 36120347; PMCID: PMC9475176. doi:10.3389/fphar.2022.939317
45. Belcher JD, Chen C, Nguyen J, et al. The fucosylation inhibitor, 2-fluorofucose, inhibits vaso-occlusion, leukocyte-endothelium interactions and NF-κB activation in transgenic sickle mice. *PLoS One*. 2015;10(2):e0117772. PMID: 25706118; PMCID: PMC4338063. doi:10.1371/journal.pone.0117772